

MINERALOGY OF MAGNETIC SOILS AT A UXO REMEDIATION SITE IN KAHO'OLAWE HAWAII

*Remke L. Van Dam¹, J. Bruce J. Harrison¹, Jan M.H. Hendrickx¹, Deidre A. Hirschfeld¹, Ryan E. North²,
Janet E. Simms², Yaoguo Li³*

¹ *New Mexico Tech, Socorro, USA*

² *US Army ERDC, Vicksburg, USA*

³ *Colorado School of Mines, Golden, USA*

Abstract

Magnetic characteristics of soils can have a profound influence on electromagnetic sensors for the detection of unexploded ordnance (UXO) and may cause false alarms in the case of spatially variable concentrations. In particular, the performance of several electromagnetic sensors is hampered by viscous remanent magnetism, which is caused by the presence of ferrimagnetic iron oxide minerals of different sizes and shapes. Tropical soils formed on basaltic substrates commonly have large concentrations of iron oxide minerals. To improve detection and discrimination of UXO in these soils it is crucial to have a better understanding of the types of minerals responsible for the magnetic behavior, as well as their distribution in space. In this paper we present the results of recent field and laboratory studies of soil magnetic properties and soil mineralogy at the former Naval training range on Kaho'olawe Island, Hawaii. We discuss the role of environmental controls such as parent material, age and precipitation on the magnetic properties.

Introduction

Many techniques have been developed for processing electromagnetic (EM) and magnetic data to discriminate UXO from non-UXO, but their performance degrades significantly at sites with magnetic soils and rocks. In an environment with highly magnetic soil, magnetic and electromagnetic sensors often detect large anomalies that are of geologic, rather than metallic, origin (Butler, 2003). Improved detection and discrimination performance will only be realized when it is understood how magnetic soil material interacts with sensors. Also it is crucial to understand the magnetic characteristics of each specific survey area and to develop techniques that utilize this information in the data processing algorithms. To meet these challenges we are pursuing a multidisciplinary research project with the objectives of (i) understanding the geologic origins and physics of soil magnetization, (ii) developing protocols and practical procedures for characterizing site magnetization (iii) developing methods for removing the effects of soil responses from magnetic measurements, and (iv) developing procedures for preprocessing electromagnetic data. The project consists of field surveys and soil sampling campaigns at four UXO sites, laboratory measurements of soil samples, and development of numerical techniques for data processing and analysis. The four UXO sites include (i) the Navy QA Grid on Kaho'olawe Island, Hawaii, (ii) The former Waikoloa Maneuver Area in Waimea and Waikoloa, the Big Island, Hawaii, (iii) the Limestone Hills and Chevallier Ranch UXO sites in Helena Valley, Montana, and (iv) the Jeep and Demo Range at the Former Lowry Bombing and Gunnery Range in Arapahoe County, Colorado.

This paper presents results of the field campaign in Kaho'olawe, Hawaii. The island was used for military training and target practice from 1941 to 1993. Despite extensive cleanup operations by the U.S.

Navy, large parts of the island are still not cleared. The magnetic properties of the Kaho'olawe geology and soils have been responsible for a large number (over 30%) of false positives in previous UXO detection surveys (Putnam, 2001). The objective of the Kaho'olawe data collection was to understand the origin and mineralogy of magnetic soil, characterize its frequency dependence and spatial variation, and quantify their effects on geophysical measurements for UXO detection and discrimination. The focus in this paper is on the lateral and vertical variation of the magnetic susceptibility, and the soil characteristics and mineralogy.

Magnetic properties of tropical soils

Tropical soils contain typically significant amounts of Hematite, α -Fe₂O₃, and Magnetite, Fe₃O₄, or Maghemite, γ -Fe₂O₃. These and other minerals can be both pedogenic (i.e., a product of soil formation) and lithogenic (i.e., unweathered minerals from the parent material). The magnetic behavior of these soils is dominated by the presence of ferrimagnetic minerals such as Magnetite and Maghemite, and to a lesser degree by Pyrrhotite (Table 1). The source of iron oxides in soils are iron-bearing minerals in the earth crust or lithosphere. The primary lithogenic iron oxides in magmatic rocks are Magnetite, Fe₃O₄, Titanomagnetite, Fe_{3-x}Ti_xO₄, and Ilmenite, FeTiO₃. However, iron is also found in Silicates and Sulfide minerals (Cornell and Schwertmann, 2003). The average magnetite and ilmenite content of tholeiitic and alkali olivine basalts, characteristic for Kaho'olawe (Clague and Dalrymple, 1987), lies between 37-46 and 24-50 g/kg (Wedepohl, 1969).

Table 1. Magnetic susceptibilities (χ) for several lithogenic and pedogenic iron oxides and soil constituents. Data from Thomson and Oldfield (1986) and Cornell and Schwertmann (2003).

Material	Chemical formula	Magnetic status	χ (10^{-8} m ³ kg ⁻¹)
Water	H ₂ O	Diamagnetic	-0.9
Quartz	SiO ₂	Diamagnetic	-0.6
Pyrite	FeS ₂	Paramagnetic	30
Ferrihydrite	5Fe ₂ O ₃ ·9H ₂ O ¹	Paramagnetic	40
Lepidocrocite	γ -FeO·OH	Paramagnetic	70
Ilmenite	FeTiO ₃	Superparamagnetic	200
Hematite	α -Fe ₂ O ₃	Antiferromagnetic	60
Goethite	α -FeO·OH	Antiferromagnetic	70
Pyrrhotite	Fe _{7/8/9} S _{8/9/10}	Ferrimagnetic	~5,000
Maghemite	γ -Fe ₂ O ₃	Ferrimagnetic	40,000
Magnetite	Fe ₃ O ₄	Ferrimagnetic	50,000

¹The amount of OH and H₂O is variable (Cornell and Schwertmann, 2003).

The concentration and type of iron oxides in soils is not only affected by the mineralogy of the parent material, but also by soil age, soil forming processes, biological activity, and soil temperature (Kitayama et al., 1997; Singer et al., 1996; Van Dam et al., 2004). The weathering of parent material leads to the release of Fe into surface environments, where it will form pedogenic iron oxides. The thermodynamic stability of an iron oxide under the particular soil conditions determines if a mineral will persist for a long time or whether it will transform into a more stable mineral. Magnetite and Ilmenite are among the most stable lithogenic iron oxides, which explains why the coarse fraction of tropical soils

often contain significant amounts of these minerals. Overall, the iron oxide content in tropical soils may be as high as several hundred g/kg (Goulart et al., 1998).

Table 1 shows the magnetic status and magnetic susceptibilities for several iron- and iron-titanium-oxides, iron-sulfides and other soil constituents. Water and quartz are diamagnetic and have a small negative magnetic susceptibility. Hydrated iron oxides like Goethite, which is the most abundant iron oxide in soils around the world, Ferrihydrite, and Lepidocrocite play a minor role in determining the magnetic character of soils. Also Hematite, which is the most abundant iron oxide in tropical soils, Pyrite, and Ilmenite hardly affect the magnetic soil characteristics. As follows from Table 1, the magnetic character of a soil is dominated by the combined amount of lithogenic and pedogenic ferrimagnetic Magnetite and Maghemite minerals in a soil (Ward, 1990).

Methods and materials

Setting

Kaho'olawe is the smallest of the eight major islands in the state of Hawaii and lies approximately 7 miles southwest of Maui (Fig. 1A). It is one of the smallest single-shield volcanoes of the Hawaiian Islands and is 1-2 million years old (Wood and Kienle, 1990). The rocks consist of tholeiitic and alkalic basalt of shield and capping stages (Clague and Dalrymple, 1987). Kaho'olawe has not erupted in historic time and is considered to be extinct. Due to its position on the leeward side of Haleakala Volcano on Maui and its limited elevation (maximum 450 meters) Kaho'olawe receives very little rainfall throughout the year. The annual rainfall is estimated to range from 250 to 600 millimeters (USDA, 1995). Overgrazing by cattle that were first introduced in 1864 has caused large areas of the island to be stripped of vegetation. The bare surface and the strong trade winds from the east have led to severe soil erosion. The sparse vegetation of the central plateau consists of piligrass and kiawe trees.

The Navy QA Grid that was selected for the geophysical measurements lies in the Kunaka/Na'alapa province (Fig. 1B) and is dominated by soils of the Kaneloa Series and Puu Moiwi Series (USDA, 1995). The parent material of these soils is strongly weathered volcanic ash over strongly weathered basic igneous rock. The Kaneloa soils reach saprolite (weathered bedrock) within 40 to 75 centimeters from the surface, while the Puu Moiwi soils have a deeper soil cover. The soil colors range from reddish brown to brown for the Puu Moiwi soils and from brown to yellowish brown for the Kaneloa soils. For both soils the texture is mostly silty clay loam and both contain detectable amounts of Hematite and magnetite at all depths (USDA, 1995).

Sampling strategy

Four soil pits that represent the variation in magnetic properties of the site were excavated in and around the test plot 2E (Fig. 1C). The locations were selected based on previously collected time-domain electromagnetic (TEM) data (Putnam, 2001), TEM data collected in this field campaign (Walker et al., This issue), and on geomorphological characteristics of the terrain. Soil pit A was located in the area with the lowest magnetic background, just outside the 2E Grid, while soil pit B was dug in the area with the highest magnetic background readings. Soil pit C was dug in an area with intermediate magnetic readings. Soil pit D was dug at a distance of approximately 75 meters south of the Grid 2E in a topographic low. For all pits the soil profiles were divided in separate horizons. After description of the horizon characteristics in the field, samples were collected for laboratory analyses of soil texture and mineralogy and frequency dependent magnetic properties. A total number of 50 soil and 2 rock samples were collected from the soil pits. The magnetic susceptibility was measured at vertical increments of 5 centimeter using a Bartington MS2 system at frequencies of 0.958 kHz (D-sensor) and 0.58 kHz (F-sensor).

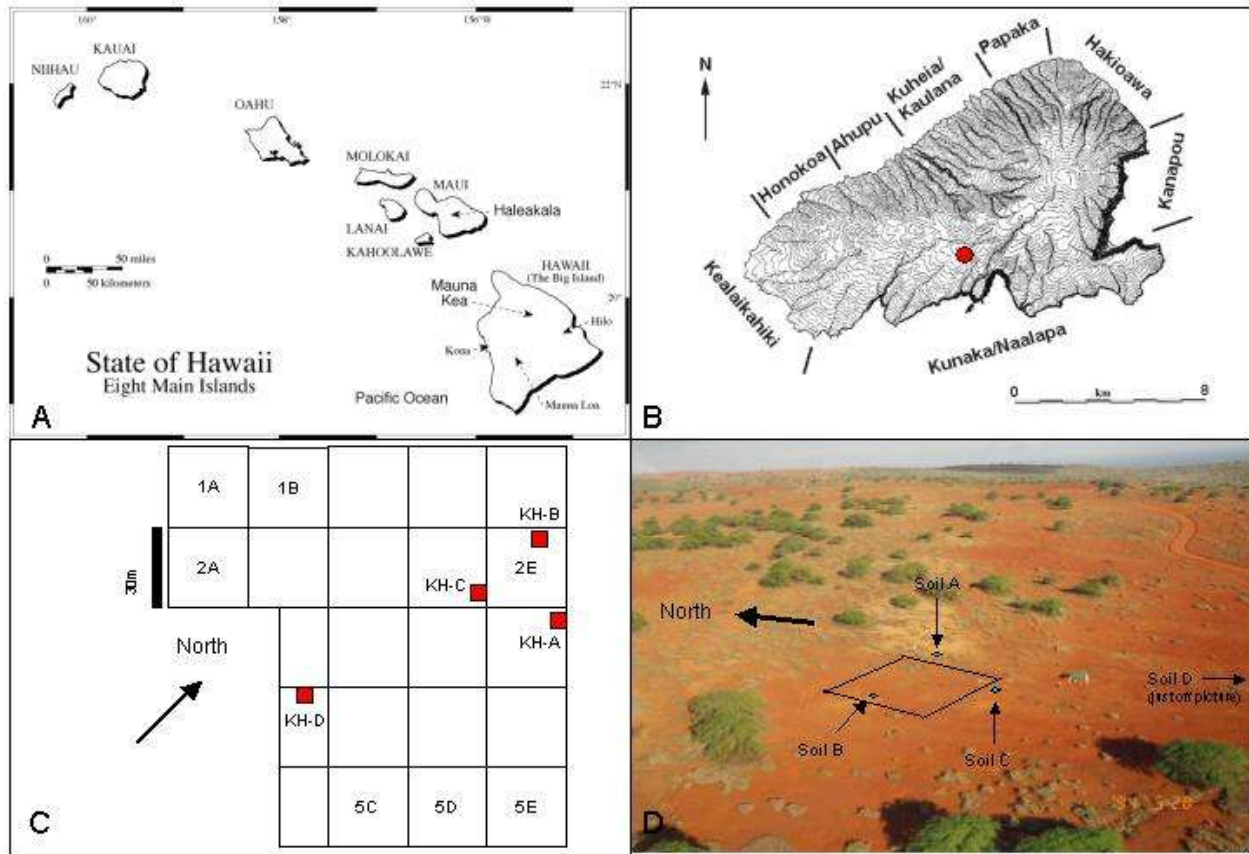


Figure 1. Location and setting of the field area. A) The eight main Hawaiian islands. B) Detailed map of Kaho'olawe with the approximate location of the field site given by the circle. C) Outline of the Navy QA Grid and locations of the four soil pits. D) Aerial photograph of the field site with the locations of test grid 2E and the soil pits.

The 30x30 meter 2E Grid that is located within the Navy QA area was subdivided in regular 5x5 meter cells. A random number generator was used to select one sampling location in each cell. This stratified random sampling strategy ensures a good coverage of the entire plot (Webster and Oliver, 1990). At each of the 36 locations the magnetic susceptibility was measured using a Bartington MS2 system at a frequency of 0.958 kHz. Also, a frequency-domain Geonics EM-38 system was used to measure the inphase and quadrature components of the magnetic responses of the soil. Finally, at each of the 36 locations, surface samples were collected for laboratory analysis of soil mineralogy and frequency dependent magnetic properties.

X-Ray Diffraction (XRD)

XRD can be used to identify the different minerals present in a sample. An X-Ray diffraction spectrum is a plot of observed diffraction intensity, related to the amount of interference between the emitted radiation and the atom structure of the sample. It allows for the identification of polymorphic iron oxides (for example α -Fe₂O₃, Hematite, and γ -Fe₂O₃, Maghemite). However, because of overlapping peaks in the resulting spectrum it is very difficult to make the distinction between lithogenic magnetite (Fe₃O₄) and pedogenic Maghemite (γ -Fe₂O₃). Also, XRD cannot be used to identify very low-crystalline minerals such as Ferrihydrite (Fe₅HO₈·4H₂O). The drawback of XRD analysis is the inherently qualitative nature of the technique. Therefore, XRD analyses are usually performed in combination with X-Ray Fluorescence Spectroscopy (XRF) to quantify the amounts of Fe and other elements.

Thermogravimetry

Thermal analysis refers to the study of the behavior of materials as a function of temperature change. Thermogravimetric analysis (TGA) measures the change in weight of a sample as a function of temperature. Differential thermal analysis (DTA) measures the temperature difference between a reference material and the sample during heat up or cool down. The shape of the TGA and DTA curves gives information on sample composition, thermal characteristics of the sample, and on the products formed during heating (Blazek, 1973). In the TGA curve, sections with zero slope indicate where the sample is stable for a certain temperature range. Nonzero slopes give the rate and direction of the weight change. The derivative (DTG) of the thermogravimetric curve shows the change in weight with time as a function of temperature or time. In DTA curves, the temperature difference between the sample and the reference material is an indication of the type (endothermic or exothermic reaction or phase change) and magnitude of the event that is occurring in the sample.

To conduct the measurements, a sample of the test material is placed into a special shape cup made of high purity alumina. An identical cup, filled with inert Al_2O_3 powder, is placed immediately beside the sample cup. When both cups are heated at the same rate, the temperature difference observed in thermocouples in the bottom of the cups is related to heat capacity differences between the sample and reference material. The DTA signal is this difference in temperature (measured in milliVolts) and is constantly saved on the computer along with the temperature inside the reference cup and the elapsed time. Several factors such as the heating rate, amount of sample, and particle size, play a role in the shape of the curves and the magnitude of events. With faster heating rates, the events tend to be broader and the peaks occur later (i.e., at higher temperatures). Similarly, smaller amounts of sample and finer grain sizes cause processes to occur faster, which leads to narrower peaks at slightly lower temperatures. These effects make it difficult to compare results from different studies.

Two samples, representative for the soils KH-A and KH-B, respectively, have been selected for thermogravimetric analysis. The measurements have been carried out from room temperature up to 1515°C results at a constant heating rate of 10 degrees per minute.

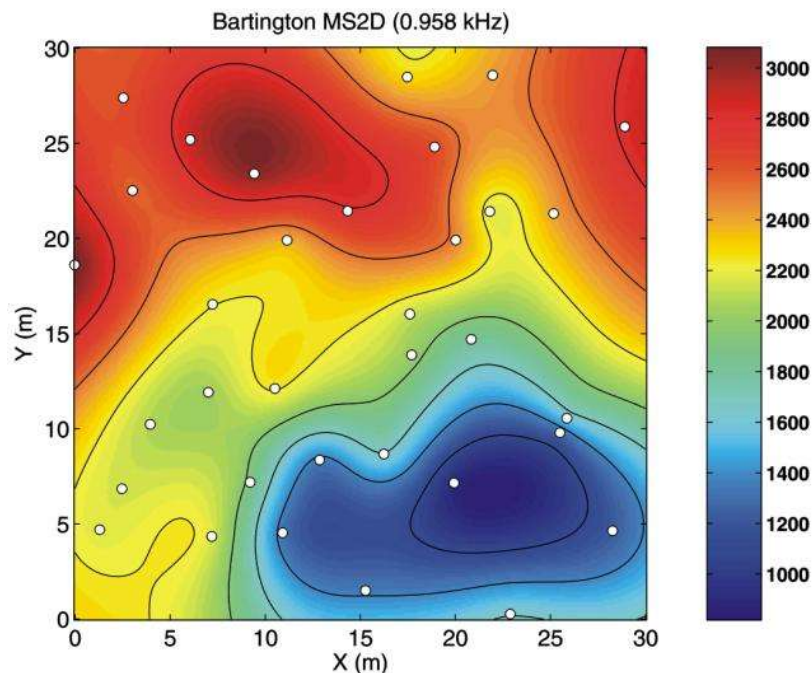


Figure 2. Soil susceptibilities in 10^{-5}SI measured in the field using Bartington MS2D sensor. The dots indicate the measurement locations. The north is to the upper right hand corner of the plot.

Results

Surface variability in magnetic susceptibility

The surface variability in magnetic susceptibility was measured at 36 locations in the grid using a Bartington MS2D sensor at a frequency of 0.958 kHz. A contour plot of the susceptibility (Fig. 2) indicates a change from high values in the west and north of the grid to lower values in the east to southeast. The region of large susceptibility corresponds to the area with a high TEM signal strength (Walker et al., This issue).

Soil descriptions

Three kinds of symbols are used in combination to designate horizons and layers. Capital letters are used to designate master horizons. A horizons are characterized by an accumulation of humified organic matter, mixed with the mineral fraction. B horizons are dominated by obliteration of all or much of the original rock structure and accumulation of a.o., clay and iron oxides (Driessen and Dudal, 1991). The C horizon is a layer that is little affected by pedogenic processes. Lower case letters, used to indicate specific horizon characteristics include: “c”, concretions or nodules with iron, aluminum, manganese or titanium cement, “w”, development of color or structure in a horizon but with little or no apparent illuvial accumulation of material, and “ox/r”, weathered or soft bedrock. In addition to the capital and lower case letters, arabic numerals are used as suffixes to indicate vertical subdivisions within a horizon and as prefixes to indicate discontinuities. Soil colors are described according to the Munsell soil color charts that organize soil colors according to their hue, value and chroma (codes between brackets in Tables 2 and 3; e.g., Cornell and Schwertmann, 2003).

The soil in pit B (KH-B), the only one located within the 2E Grid, has the highest magnetic susceptibility readings of any site. The soil is very similar to KH-C and KH-D although the upper horizon appears more purple colored, perhaps indicating a higher Hematite content. Six horizons were identified, most of which are horizons in which all or much of the original rock has been very strongly weathered (Fig. 3). There is no strong indication of clay translocation in the soil. Originally, these horizons have been formed under an A horizon, characterized by the accumulation of organic matter. Its absence demonstrates the erosive history of the soil. Starting from a depth of around 0.4 meters the red color of the soil gradually changes into a more yellow color (Table 2). Below 1.1 meter depth the amount of partly unweathered parent material in the soil increases.

Table 2. Description of Soil KH-B.

Bw1 0 to 5cm	Dark red (10R 3/6) silty clay loam, weak red (10R 4/4) moist; strong coarse angular blocky to strong fine subangular blocky; hard, slightly sticky, slightly plastic; boundary clear wavy.
Bw2 5 to 15cm	Dark red (10R 3/6) silty clay loam, dark reddish brown (2.5YR 3/4) moist; strong medium angular blocky to strong fine subangular blocky; hard, slightly sticky, slightly plastic; boundary clear wavy.
Bw3 15 to 40 cm	Red (10R 4/6) silty clay loam, red (2.5YR 4/6) moist; massive; hard, slightly sticky, slightly plastic; boundary clear wavy.
Bw4 40 to 70cm	Red (2.5YR 4/6) loam, dark reddish brown (2.5YR 3/4) moist; massive; slightly hard, very slightly sticky, slightly plastic; boundary gradual wavy; fungal hyphae, iron oxides along ped faces.
Bw5 70 to 110cm	Yellowish red (5YR 5/8) loam, dark reddish brown (2.5YR 3/4) moist; massive; slightly hard, nonsticky, nonplastic; boundary gradual wavy; fungal hyphae, iron oxides along ped faces; 2cm thick layer with some white/grey saprolite rock/pebbles at 90cm depth.
Bw/Cox 110 to 130cm	Yellowish red (5YR 5/8) loam, yellowish red (5YR 4/6) moist; massive; slightly hard, nonsticky, nonplastic.

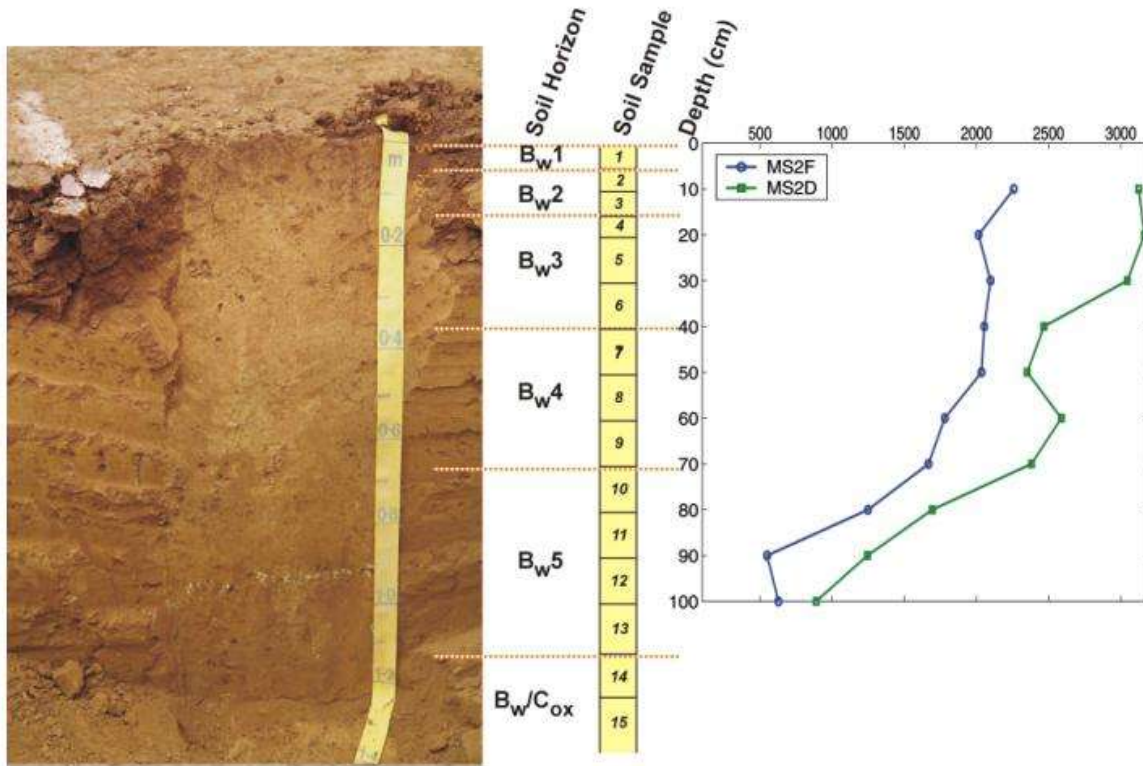


Figure 3. A picture of the soil profile KH-B in Pit B, the soil horizons, and the sampling locations. The graph shows the susceptibility values (in 10^{-5} SI) measured with the Bartington MS2D (0.958 kHz) and MS2F (0.58 kHz) sensors. The Bartington data have not been corrected for inter-sensor variability.

The soil in pit A (KH-A) is located in an area of low magnetic background (TEM) and magnetic susceptibility (Bartington) readings. The area has been significantly eroded. Bedrock is found within 40 cm of the surface (Fig. 4). A very thin remnant of a reddish lower B horizon lies directly over Cox (Table 3). The surface color at this site is yellowish to dark grey to green (Fig. 1D), similar to what is seen at depth in the bedrock. The entire soil profile is dominated by partly weathered basalt or saprolite. The Cox1 and Cox2 horizons below the Bw/Cox horizon are characterized by increasing amounts of saprolite. This soil, at the highest elevation of the four soil pits, has been subject to more severe erosion than the other soils. Before the erosion started, the Bw/Cox horizon that is exposed here at the surface, was located below A and B horizons in the profile.

Table 3. Description of Soil KH-A.

Bw/Cox 0 to 10cm	Dark reddish brown (5YR 3/3) silty clay loam, dark brown (7.5YR 3/4) moist; strong medium subangular blocky; slightly hard, slightly sticky, slightly plastic; boundary gradual wavy.
Cox1 10 to 40cm	Increasing amount of weathered bedrock; fill in fractures is yellowish brown (10YR 5/6) silty clay loam, dark yellowish brown (10YR 4/6) moist; nonsticky and nonplastic; boundary gradual wavy.
Cox2 40 to 110cm	similar texture to above; amount of weathered basalt (pseudomorphs) increased; degree of induration of basalt increased; significant weathering occurring along fractures; weathering occurring along fractures in basalt, color varies from dark purple to grey to green.

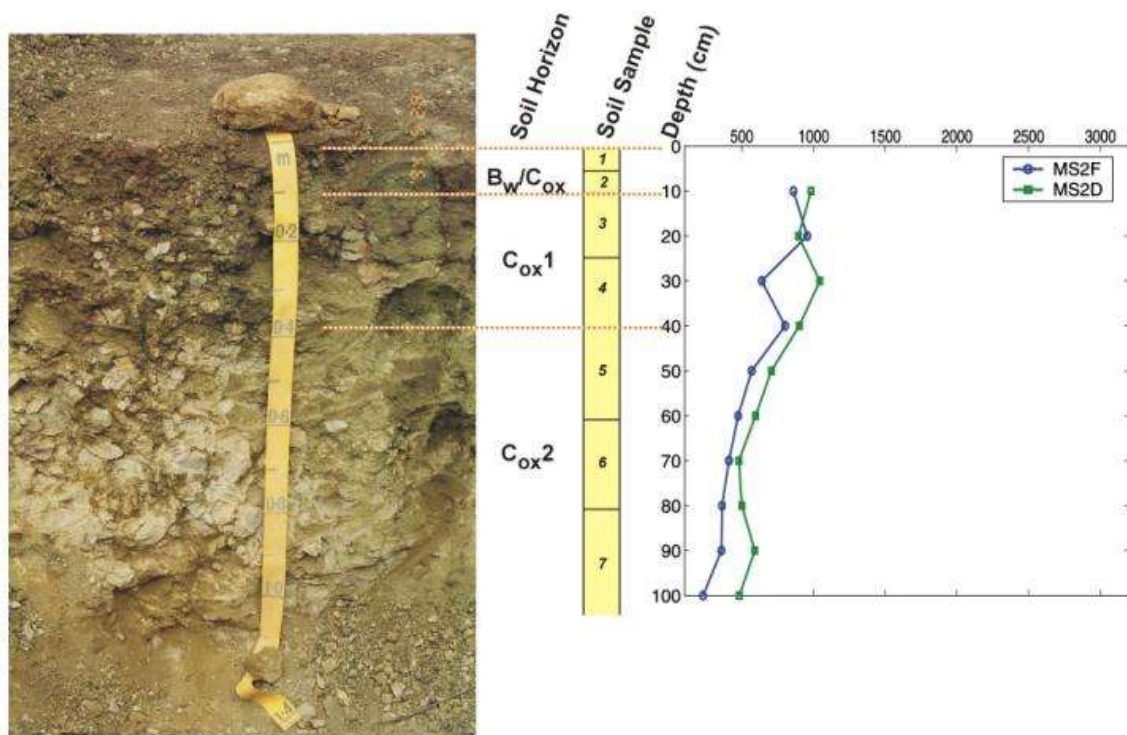


Figure 4. A picture of soil profile KH-A in Pit A, the identified soil horizons, and sampling locations. The graph shows the susceptibility values (in 10^{-5} SI) measured with the Bartington MS2D (0.958 kHz) and MS2F (0.58 kHz) sensors. The data have not been corrected for inter-sensor variability.

Soil magnetic properties

The Bartington measurements indicate a very large magnetic susceptibility in the top horizons of soil KH-B (Fig. 3). Below a depth of 0.7 meters the magnetic susceptibility decreases significantly. A trend of decreasing magnetic susceptibility values with depth is in agreement with observations in earlier studies (Singer et al., 1996; Van Dam et al., 2004). In soil KH-A the magnetic susceptibility values are much lower than those in soil KH-B. In the top horizon of soil KH-A the susceptibility values are around $1000 \cdot 10^{-5}$ SI (Fig. 4), similar to those at 1 meter depth in soil KH-B. With increasing depth in soil KH-A, the magnetic susceptibility decreases further. The magnetic susceptibility values (measured with the D-sensor) for the top horizons (Bw) in Pits A and B (1000 and $3000 \cdot 10^{-5}$ SI, respectively) are consistent with those observed in the surface measurements (Fig. 2).

X-Ray Diffraction (XRD)

Four soil samples from different depths in the soil pits A and B have been analyzed using XRD (Table 4). Soil A is characterized by the abundance of numerous minerals at all depths in the profile. Kaolinite is only present in the top 2 samples. Gibbsite is clearly present in all samples, except for sample KH-A3 where only an indication of the mineral was found. Soil B is dominated by iron oxide minerals Goethite, Hematite, and Magnetite in the top three samples. The lowermost sample from the Bw/Cox horizon has several characteristics of the material in soil A: both Gibbsite and Muscovite are present and only an indication of the presence of Hematite and Magnetite is found. The yellowish color of soil A and the Bw/Cox horizon in Soil B is possibly caused by the presence of Gibbsite (USDA, 1995). However, Goethite is usually thought to be responsible for a yellowish soil color (Cornell and Schwertmann, 2003). In this case, the smaller amount of red-coloring Hematite in the majority of the samples from soil A and the lowest sample in soil B, may contribute to the yellower color.

Table 4. Results of XRD analyses of selected samples from Soil A and B. The symbol “x” denotes a clear presence of the particular mineral, while the symbol “o” denotes an indication of the mineral's presence. In the latter case, a small amount of the mineral-specific peaks does not overlap with the peaks in the X-ray spectrum for the sample.

Sample	Depth (m)	Horizon	Goethite α -FeOOH	Hematite α -Fe ₂ O ₃	Magnetite Fe ₃ O ₄	Ilmenite FeTiO ₃	Gibbsite Al(OH) ₃	Muscovite (Mica's)	Kaolinite
KH-A1	0-0.05	Bw/Cox	x	x	x	x	x	x	x
KH-A3	0.1-0.25	Cox1	x	o	x	x	o	x	o
KH-A5	0.4-0.6	Cox2	x	o	x	x	x	x	
KH-A7	0.8-1.1	Cox2	x	o	x	x	x	x	
KH-B1	0-0.05	Bw1	x	x	x				
KH-B5	0.2-0.3	Bw3	x	x	x				
KH-B8	0.5-0.6	Bw4	x	x	x				
KH-B15	1.2-1.3	Bw/Cox	x	o	o		x	x	

Thermogravimetry

Thermal analysis has been used to analyze one sample from each soil; KH-A3 from a depth of 0.1 to 0.25m in horizon Cox1 of soil A, and KH-B5 from a depth of 0.2 to 0.3m in horizon Bw3 of soil B. The TGA curves show a number of clear weight loss events that can be recognized for both samples, around 100, 300, 450-500, and 1400-1450°C (Fig. 5). The DTA curves show events at similar temperatures, but indicate the presence of two extra events at around 80°C in sample KH-B5 and at 900°C in sample KH-A3. In the DTA curves negative peaks denote endothermic reactions (i.e., consuming heat) while positive peaks indicate exothermic reactions (i.e., giving off heat).

In Table 5, the observed events are correlated with literature data on thermal behavior of soil material (Blazek, 1973; Földvari, 1991; Van Dam, 2002). The TGA curves show a strong weight loss between the start of the measurements and 120°C with a DTA peak at around 110°C. This is caused by the evaporation of free water from the pores. The exothermic reaction at 80°C in sample KH-B5 is difficult to explain. This effect is possibly due to the presence of a small amount of organic material in the sample. The endothermic effect at around 280°C occurs in both samples. This event may be related to the dehydroxylation of Gibbsite, as suggested by Blazek (1973) and Földvari (1991). However, the XRD analysis suggests that Gibbsite is present only in sample KH-A3 (Table 4). Therefore, this effect is probably at least partly due to the dehydroxylation of Goethite (Van Dam et al., 2002) and other minerals with “-H₂O” groups. The weight loss event at around 500°C is possibly caused by loss of structural water from Kaolin and/or Mica type clay minerals. Both the TGA and DTA curves indicate that this event is larger in sample KH-A3 than in sample KH-B5. This observation is supported by the difference in clay minerals found using the XRD analysis (Table 4).

Between about 600 and 1400°C the TGA weight loss is negligible. Nevertheless, the DTA curves indicate several processes. The exothermic effect in sample KH-A3 at 900°C is most probably caused by a chemical or structural change in the clay mineral Kaolinite or Muscovite. From 900°C onwards the DTA curves show a downward slope, which indicates an endothermic reaction. This downward sloping curve culminates in a sharp drop around 1380°C, which is the result of the melting of Hematite (Blazek, 1973). The drop is largest in sample KH-B5, which is expected to have the largest amount of Hematite (Table 4).

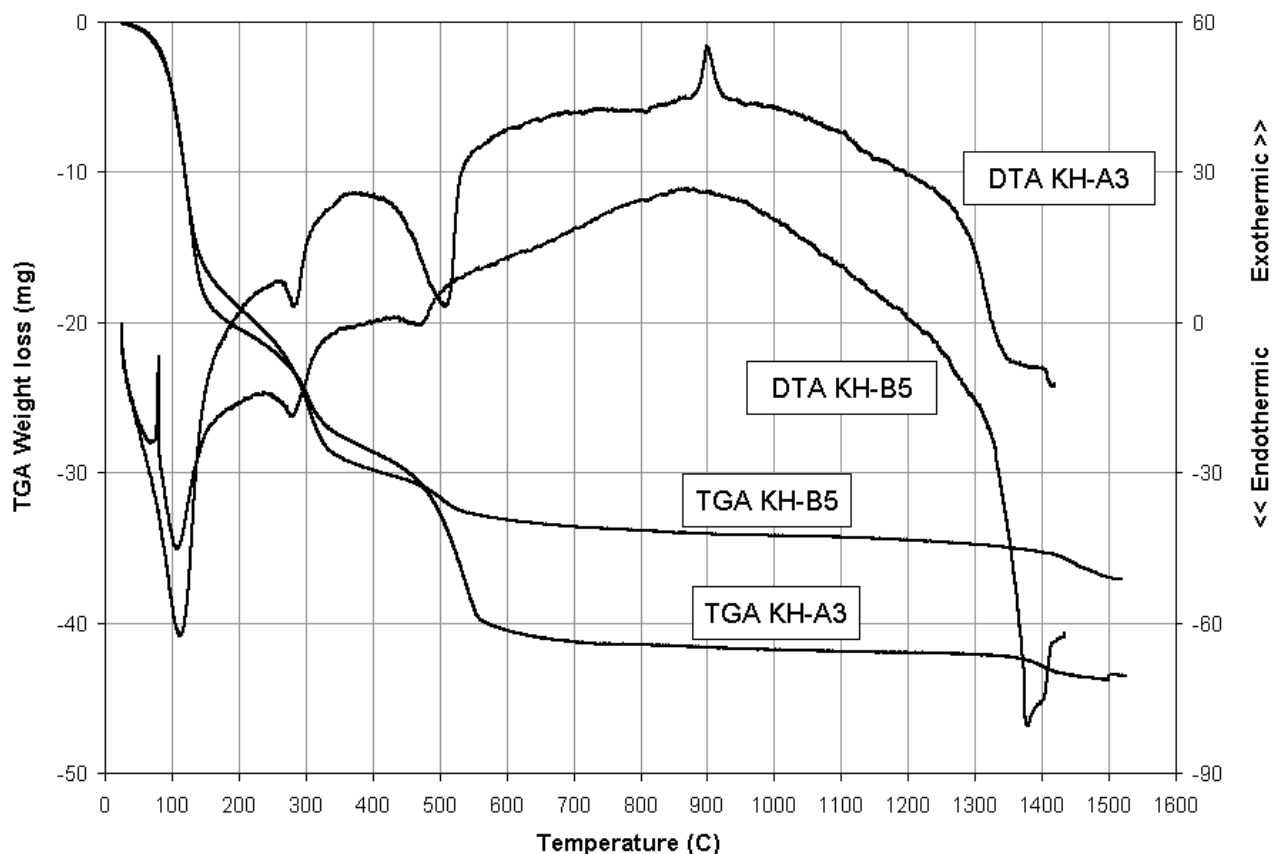


Figure 5. TGA and DTA curves for two samples from soil KH-A and KH-B.

Table 5. Comparison of TGA and DTA with events described in literature.

DTA peak temperature (°C)	Reaction type	Sample KH-A3	Sample KH-A5	Probable effect	Temperature (°C)
80	Exothermic		DTA	Organic material	
110	Endothermic	TGA,DTA	TGA,DTA	Loss of free water	~100
280	Endothermic	TGA,DTA	TGA,DTA	Dehydration of Gibbsite and formation of böhmite ¹	250-330
				Dehydroxilation of Gibbsite ²	270-380
				Dehydroxilation of Goethite ³	280
470	Endothermic		TGA,DTA	Decomposition of böhmite (γ -AlO·OH) ¹	
				Loss of structural water from Kaolin or Micas ¹	
510	Endothermic	TGA,DTA		Decomposition of böhmite (γ -AlO·OH) ¹	
				Loss of structural water from Kaolin or Micas ¹	
900	Exothermic	DTA		Chemical or structural change in Kaolinite or Mica (Muscovite) ¹	
~1380	Endothermic	TGA,DTA	TGA,DTA	Hematite melting ¹	1360-1440

¹ Blazek (1973), ² Földvari (1991), ³ Van Dam (2002)

Discussion and Conclusions

This paper deals with the mineralogical causes of magnetic behavior of soils in Kaho'olawe, Hawaii. The origin of the magnetic minerals in the soils is primarily the tholeiitic and alkali basalt parent material. However, soil formation plays an important role in enhancing the magnetic character of the soils. This follows from the fact that Soil A, which has undergone significant erosion and where the depth-to-bedrock is the smallest, the magnetic signal is smaller than in soil B (Figs. 3 and 4). Iron is a major component of many minerals in the basaltic parent materials such as Magnetite, Titanomagnetite, and Ilmenite.

The results from the studies in Kaho'olawe demonstrate the relative enrichment with magnetic minerals due to soil forming processes. The XRD laboratory analyses show that some primary-rock minerals still persist in the soils (Ilmenite in KH-A3), while several newly formed iron oxides are present as well, especially in KH-B5. The XRD analysis also points to the presence of (lithogenic) Magnetite or (pedogenic) Maghemite. Due to the limitations of the technique, the XRD analysis can not be used to distinguish between the two minerals. The thermogravimetric analysis is not conclusive either. Maghemite is expected to produce an exothermic reaction between 510 and 570°C, but this information is based on synthetic sample material only (Blazek, 1979). Magnetite is expected to produce an exothermic reaction between 590 and 650°C. Possibly, the exothermic trend between 500 and 850°C in the DTA curve of soil sample KH-B5 is related to this effect. More research is needed, and planned, to study this effect.

Wind erosion of soil material plays a major role in the distribution of magnetic properties in the Navy QA Grid on Kaho'olawe. The amount of erosion seems to be well predicted by the color of the soil surface. Soils that are yellow from the surface indicate that the majority of the Bw horizon material has been eroded. Soils that are reddish at the surface are less severely eroded and have retained some of the more highly magnetic material in the Bw horizons. It is anticipated that the soil map of Kaho'olawe (USDA, 1995) can be used in combination with IKONOS or SPOT satellite images to predict the magnetic background signal for large areas on Kaho'olawe's windswept central plateau.

Additional research is needed to disentangle the complex soil mineralogical web and to get a clearer picture of the specific minerals responsible for the magnetic behavior of the soils at Kaho'olawe. It is scheduled to perform additional XRD and thermogravimetric analysis on more samples from the soil pits. Also, we will perform XRF measurements on all soil samples. It is scheduled to use two differential dissolution methods (Na dithionite, Fe_d, and NH₄-oxalate, Fe_o) that can be used to estimate the maturity of the soils.

References

- Blazek, A., 1973, Thermal Analysis. Van Nostrand Reinhold Co.
- Butler, D.K., 2003, Implications of magnetic backgrounds for unexploded ordnance detection, *Journal of Applied Geophysics*, 54, pp.111-125.
- Clague, D.A., and Dalrymple, G.B., 1987, The Hawaiian-Emperor volcanic chain Part II, in *Volcanism in Hawaii*, R.W. Decker, T.L. Wright, and P.H. Stauffer, eds., U.S. Geological Survey Professional Paper 1350, 1, pp.5-54.
- Cornell, R.M. and Schwertmann, U., 2003, *The iron oxides: structure, properties, reactions, occurrences and uses*. Wiley-VCH.
- Driessen, P.M. and Dudal, M., 1991, *The major soils of the world*. Koninklijke Wöhrmann B.V.

- Földvari, M., 1991, Measurement of different water species in minerals by means of thermal derivatography, in *Thermal Analysis in Geosciences*, W. Smykatz-Kloss and S.S.J. Warne, eds. Springer-Verlag Berlin.
- Goulart, A.T., Fabris, J.D., De Jesus Filho, M.F., Coey, J.M.D., Da Costa, G.M., and De Grave, E., 1998, Iron oxides in a soil developed from basalt, *Clays and Clay Minerals*, 46, pp.369-378.
- Kitayama, K., Schuur, E.A.G., Drake, D.R., and Mueller-Dombois, D., 1997, Fate of a wet montane forest during soil aging in Hawaii, *Journal of Ecology*, 85, pp.669-679.
- Mullins, C.E., 1977, Magnetic susceptibility of the soil and its significance in soil science - a review, *Journal of Soil Science*, 28, pp.223-246.
- Putnam, J., 2001, Kaho'olawe program management and technology, in *Proceedings of The UXO/Countermines Forum*, November 27-29, Washington, D.C.
- Singer, M.J., Verosub, K.L., Fine, P., and TenPas, J., 1996, A conceptual model for the enhancement of magnetic susceptibility in soils, *Quaternary International*, 34-36, pp.243-248.
- Thompson, R. and Oldfield, F., 1986, *Environmental Magnetism*. Allen & Unwin.
- USDA, 1995, *Soil survey of the Island of Kahoolawe, Hawaii*. United States Department of Agriculture.
- Van Dam, R.L., Hendrickx, J.M.H., Harrison, B., Borchers, B., Norman, D.I., Ndur, S.A., Jasper, C., Niemeyer, P., Nartey, R., Vega, D., Calvo, L., and Simms, J.E., 2004, Spatial variability of magnetic soil properties, in *Detection and remediation technologies for mines and minelike targets VIII*, *Proceedings of the SPIE*, 5415, pp.665-676.
- Van Dam, R.L., Schlager, W., Dekkers, M.J. and Huisman, J.A., 2002, Iron oxides as a cause of GPR reflections, *Geophysics* 67(2), pp.536-545.
- Walker, S.E., Pasion, L.R., Billings, S.D., Li, Y., and Oldenburg, D.W., This issue, Examples of the effect of magnetic soil environments on time domain electromagnetic data.
- Ward, S.H., 1990, *Geotechnical and Environmental Geophysics*. Society of Exploration Geophysicists.
- Webster, R. and Oliver, M.A., 1990, *Statistical Methods in Soil and Land Resource Survey*. Oxford University Press.
- Wedepohl, K.H., 1969, Composition and abundance of common igneous rocks, in *Handbook of Geochemistry*, K.H. Wedepohl, ed. Springer-Verlag Berlin.
- Wood, C.A. and Kienle, J., 1990, *Volcanoes of North America: United States and Canada*. Cambridge University Press, New York.

Acknowledgments

We thank the Kaho'olawe Island Reserve Commission (KIRC) for permission to collect data on Kaho'olawe. The support and assistance provided by the KIRC staff was instrumental for the success of this field study. We thank Len Pasion, Sean Walker, Shinku Sky, Todd Meglich, and Mike Donaldson for assistance during the fieldwork. We thank Scott Morton for assistance with the thermogravimetric measurements and Chris McKee of the New Mexico Bureau of Geology and Mineral Resources' X-Ray Diffraction Laboratory for valuable help. The research was funded by grants from SERDP (UX-1414 and UX-1355) and ARO (STIR19-02-1-027).